

# Importance of water polarization for ion permeation in narrow pores

Denis Bucher, Serdar Kuyucak\*

School of Physics, University of Sydney, NSW 2006, Australia

## ARTICLE INFO

### Article history:

Received 8 April 2009

In final form 22 June 2009

Available online 25 June 2009

## ABSTRACT

Molecular dynamics (MD) simulations are mostly performed using non-polarizable force fields. This approximation works in homogeneous systems but there are situations – such as pores, cavities and interfaces – where an explicit description of polarization may be necessary. Here, we perform density functional calculations and Car–Parrinello MD simulations to investigate the effect of polarization on solvated ions in narrow pores. Polarization of water molecules in the first hydration shell of a  $K^+$  ion is found to be significantly larger in a narrow pore compared to that in bulk water. Implications of these observations on the energetics of ion permeation in narrow pores are discussed using simple models.

© 2009 Elsevier B.V. All rights reserved.

## 1. Introduction

Molecular dynamics (MD) simulations have been increasingly used to study properties of atomic systems. Examples range from various materials [1,2] to carbon nanotubes [3] and biomolecules [4,5]. For reasons of simplicity and computational efficiency, most MD simulations make use of non-polarizable pair-wise potentials, where the effect of polarization is included implicitly by increasing the partial charges on atoms. This mean field approximation works fairly well in homogeneous or bulk-like systems where the non-polarizable potentials are parameterized, but evidence is gathering that this is not the case in inhomogeneous systems such as pores [6–9], cavities [10,11] and interfaces [12,13]. An explicit description of polarization effects would significantly improve the transferability of force field parameters in such systems. Although much progress has been made towards that goal, a properly optimized polarizable force field with broad applicability is yet to be developed (see, e.g., Ref. [14] and the accompanying special issue on polarization). A main impediment in this regard is lack of sufficient experimental data to constrain the polarization models and the parameters they employ. *Ab initio* studies of polarization effects in appropriately chosen systems could ameliorate this situation by providing complementary information that could help to distinguish among competing models.

Water plays a key role in structure and function of biomolecules, and therefore provides a pertinent example for illustrating the problems faced by the non-polarizable force fields in description of inhomogeneous systems. The dipole moment of the water monomer in the gas phase is 1.86 D [15,16], which is boosted to 2.35 D in the non-polarizable TIP3P water model [17]. Both experiments and *ab initio* calculations indicate that the actual value of the dipole moment in bulk water is considerably larger, e.g., X-

ray and neutron diffraction experiments give  $2.9 \pm 0.6$  D [18], while Car–Parrinello MD simulations [19] yield about 3.0 D [20–22]. But what is more worrying for a fixed dipole model is that the value of the dipole moment changes with the environment, exhibiting sizable variations. An intriguing example is given by the *ab initio* calculations of the water dipole moment in the first hydration shell of ions – it is found to be reduced from the bulk value of 3.0 D to 2.8 D in  $K^+$  but increased to 3.4 D in  $Ca^{2+}$  [22]. This example highlights the important role played by the hydrogen bond network in polarizing water [23–25]. When it is disrupted, even by a monovalent cation, there is loss of polarization. Apparently the electric field of the ion is not strong enough to compensate for those of hydration waters, which are in a frustrated configuration with respect to each other.

Among the inhomogeneous systems, narrow pores provide a particularly interesting case for studying the polarization effects. Despite the disruption of the hydration shell to a single-file configuration, monovalent cations can permeate across narrow channels such as gramicidin A (gA) near diffusion rates. Non-polarizable force fields have not been able to reproduce this behavior, predicting instead a large energy barrier for an ion at the channel center [6,7]. Inclusion of polarization may resolve this problem if reduction in water polarization due to confinement is more than compensated by the favorable ion–water and water–water interactions, which would lead to larger dipole moments for water in gA compared to those in the hydration shell of an ion in bulk. Resolution of this issue will have considerable ramifications for application of classical MD simulations to inhomogeneous systems.

## 2. Computational methods

Here, we investigate this problem by performing density functional calculations and Car–Parrinello MD simulations of ion–water clusters in a carbon nanotube and gA channel (Fig. 1). The two systems are very similar geometrically, both having a radius

\* Corresponding author. Fax: +61 2 9351 7726.

E-mail address: [serdar@physics.usyd.edu.au](mailto:serdar@physics.usyd.edu.au) (S. Kuyucak).

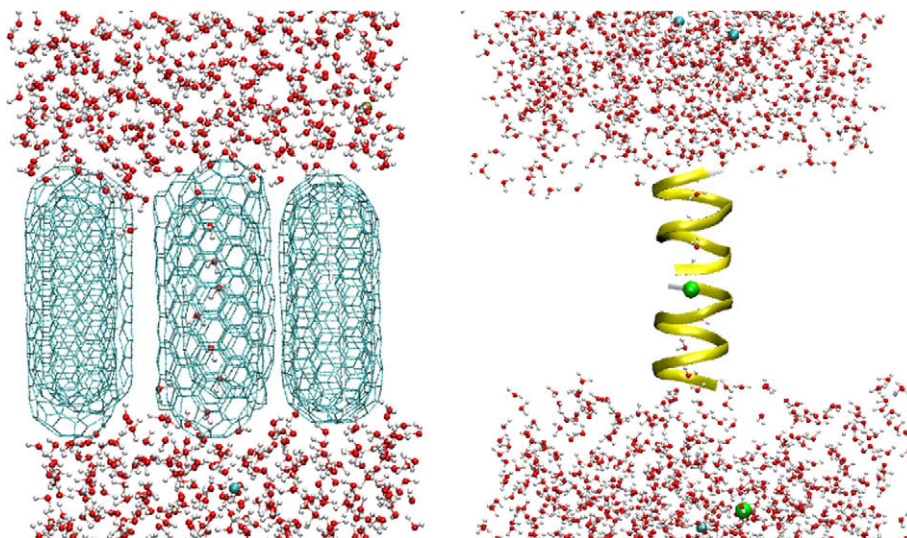


**Fig. 1.** QM/MM simulation systems: (6,6) armchair carbon nanotube (left), gA channel (right). The nanotube is surrounded by a layer of capped nanotubes while gA is embedded in a lipid bilayer (not shown). Both systems are hydrated with water. The  $K^+$  ion is at the pore center accompanied by single-file water molecules.

of about 2 Å and length 26 Å. Both can accommodate seven water molecules or an ion and six water molecules in a single-file configuration. While both pores allow water permeation, only gA conducts ions thanks to the attractive interactions with the carbonyl dipoles lining the channel wall. Thus the reason for including the carbon nanotube in this study is to assess the effect of confinement on water dipoles without the complications arising from the interactions with the charged peptide atoms. The model systems have been taken from previous MD studies [26,27], to which we refer for details. For both systems, we consider two situations: one with only water in the pore which provides a reference point, and second with a  $K^+$  ion at the center of the pore.

All four systems are initially equilibrated for 3 ns using classical MD simulations. For this purpose the NAMD code, version 2.5 [28] is used with the PARAM27 version of the CHARMM force field [29]. MD simulations are performed using an NpT ensemble with periodic boundary conditions. Pressure and temperature are kept at 1 atm and 298 K, respectively, using the Langevin coupling method with a damping coefficient of  $5 \text{ ps}^{-1}$ . Electrostatic interactions are computed using the particle-mesh Ewald algorithm. A time-step of 2 fs is employed in the MD simulations.

The *ab initio* calculations are performed using a QM/MM scheme [30], where the interior of the pore is described quantum mechanically, and the rest of the system is described at the classical level. The size of the orthorhombic QM box is typically  $20 \times 20 \times 34 \text{ Å}^3$  and contains about 250 atoms. For the carbon nanotube, the QM part consists of the carbon atoms forming the tube and the water molecules with or without a  $K^+$  ion inside. Partition of the gA system is similar with the provision that the backbone atoms forming the  $\beta$ -helix are included in the QM part but not the side chains, which are described classically. Capping hydrogen atoms are used to complete the valence of the QM/MM boundary atoms.

The quantum problem is solved using the density functional theory [31], with the BLYP functional which includes the gradient corrections [32,33]. The core-valence electron interactions are described using Martins and Trouillier pseudopotentials [34]. The Kohn–Sham orbitals are expanded in a plane-wave basis set with an energy cutoff of 80 Ry. In Car–Parrinello MD simulations [35] the fictitious electron mass is chosen to be 600 a.u. and a time-step of 0.097 fs is used.

For sampling purposes, we have created 30 snapshots for the four model systems by performing a further 3 ns of classical MD

simulations. Coordinates for the sample systems are collected at 100 ps intervals. Each system is equilibrated with QM/MM Car–Parrinello simulations for 1 ps and then the electronic structure is optimized. Dipole moments for individual water molecules are computed using the concept of Maximally Localized Wannier Functions (MLWF) analysis [36]. The MLWF orbitals are obtained from the Bloch orbitals by a unitary transformation and their spread is minimized iteratively. The centers of the MLWF's and their associated charges obtained with this procedure provide a quantitative description for the dipole moments of water molecules [20].

### 3. Water polarization in pores

The results of the water dipole moment calculations are shown in Figs. 2 and 3. The main result is summarized in Fig. 2, which compares the distribution of water dipole moments in bulk (top) with that in the gA channel (bottom). The bulk results are essentially taken from an earlier Car–Parrinello MD simulation study [22], which is extended here to get better sampling. The solid line in each graph refers to the water molecules in the first hydration shell of a  $K^+$  ion in bulk or the nearest neighbors of a centrally placed  $K^+$  ion in gA. Similarly, the dashed lines show the results obtained for the two cases in the absence of an ion. In the case of gA, the water molecules sampled are in the same positions as those with the  $K^+$  ion present (i.e., the nearest neighbors of the central water molecule).

The average dipole moments obtained from the distributions are: 3.00 D (bulk water), 2.78 D (hydration shell of  $K^+$  in bulk), 2.70 D (water in gA), and 3.05 D (hydration shell of  $K^+$  in gA). It is seen that presence of a  $K^+$  ion in bulk leads to a suppression of the water dipole moments in its immediate vicinity whereas the opposite happens in the gA channel. As discussed in the introduction, the suppression in the bulk case results from the repulsive dipole–dipole interactions among the water molecules in the first hydration shell of an ion. In contrast, the dipole–dipole interactions remain mostly attractive in gA, hence presence of an ion actually boosts the dipole moment of the neighboring water molecules. Because the ion–dipole interaction is proportional the dipole moment, it will be larger in the gA channel compared to bulk. This effect is not taken into account in the current MD force fields with fixed dipoles, which may explain the large free energy barriers found for entry of an ion from bulk to the channel center.

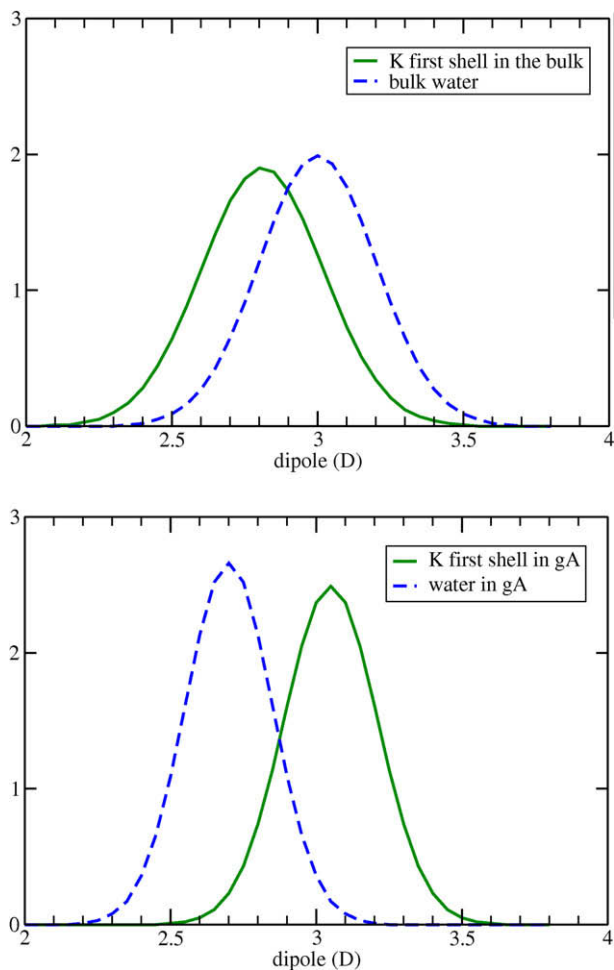


**Fig. 2.** Distribution of water dipole moments in bulk water (top) and gA (bottom). The solid lines show the dipole moments in the first hydration shell of a  $K^+$  ion and the dashed lines those of water in the absence of an ion.

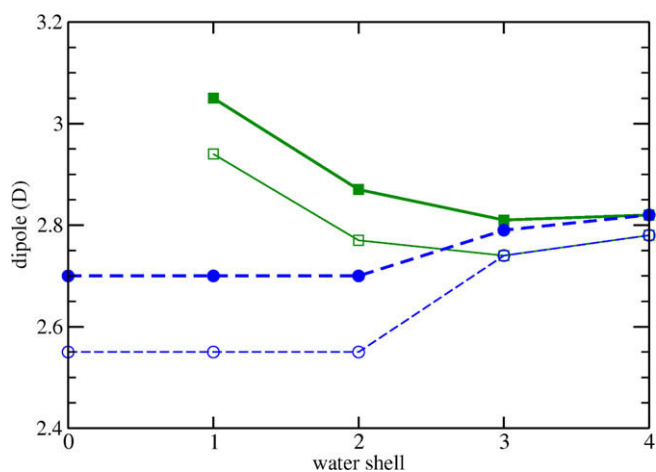


**Fig. 3.** Average water dipole moments inside the gA channel (thick lines) and the carbon nanotube (thin lines) with a  $K^+$  ion at the center (solid) and without (dashed).

The complete information on the average dipole moments of the water molecules in the four systems (gA and carbon nanotube with and without a central  $K^+$  ion) is presented in Fig. 3. Here the zeroth shell refers to the central water molecule in the pure water

cases, and the shells 1–4 indicate the position of the single-file water molecules with respect to the central ion or water molecule. When there are only waters in the channels, their dipole moments are seen to be reduced relative to the bulk value of 3.0 D. This is simply a consequence of the loss of hydrogen bonds in confined water. The most common number of hydrogen bond interactions per water molecule is four in bulk water, which is reduced to two in a water chain. Each hydrogen bond contributes about 0.2 D to the dipole moment [22,24], which explains the reduction in the dipole moment of central waters in the carbon nanotube. In the gA channel, the carbonyl groups provide an extra hydrogen bond for the water molecules – which is, though, not quite optimal – leading to a 0.15 D increase in the dipole moment values relative to those in the carbon nanotube.

An instructive exercise here is to repeat the above calculations with the channel atoms included in the MM region instead of QM, which helps to assess how much their polarization contributes to the polarization of water molecules. In the carbon nanotube, exactly the same results are obtained as before, indicating that polarizable carbon atoms are not required for description of water permeation through carbon nanotubes. In the case of gA, the dipole moment of central waters is reduced from 2.70 to 2.66 D. Thus a quarter of the 0.15 D attributed to the peptide atoms above arises from their polarization, the rest being directly induced by the peptide charges.

When a  $K^+$  ion is placed at the center of the channel, the water dipoles align with its electric field and point away from the ion. Presence of the  $K^+$  ion accentuates the cooperative effects of hydrogen bonds by forcing an alignment of water molecules and by increasing their polarization. Comparing the  $K^+$  ion results with those without the ion (Fig. 3), we see that the polarizing effect of the ion is particularly strong in the first and second hydration shells, and is dissipated only in the third shell. In contrast the polarizing effect of the ion in bulk is already dissipated by the second shell [22]. To appreciate the role of cooperative effects in the single-file configuration, it is useful to compare the dipole moment in the first shell in gA (3.05 D) and nanotube (2.95 D) with that in a single water- $K^+$  ion system in the gas phase (2.61 D) [22]. The difference between the gA and nanotube result indicates that the peptide interactions contribute about 0.10 D to the calculated dipole moment. Assuming 0.2 D contribution from the hydrogen bond with the second shell water, the remaining 0.14 D must come from the cooperative effects.

To assess the impact of water polarization on ion permeation, one needs to compute the free energy difference for translocating an ion from bulk to the channel center with QM/MM simulations. However, the sampling time required for convergence of such calculations ( $> 1$  ns [26]) renders this approach prohibitive at present. In order to give a feeling for the energies involved, we use two very simple models instead: (A)  $K^+$  is surrounded by 6 water molecules in a cubic configuration, which mimics its first shell coordination in the bulk, (B)  $K^+$  is in the middle of a chain of 6 water molecules, which mimics its configuration in the gA channel (Fig. 4). The total electrostatic energy for these models can be computed using the classical formula

$$U = \frac{-e}{4\pi\epsilon_0} \sum_i \frac{\mathbf{p}_i \cdot \hat{\mathbf{r}}_i}{r_i^2} + \frac{1}{4\pi\epsilon_0} \sum_{i>j} \frac{1}{r_{ij}^3} [\mathbf{p}_i \cdot \mathbf{p}_j - 3(\mathbf{p}_i \cdot \hat{\mathbf{r}}_{ij})(\mathbf{p}_j \cdot \hat{\mathbf{r}}_{ij})] \quad (1)$$

where  $\mathbf{p}_i$  denotes the dipoles,  $r_i$  is the ion–dipole distance and  $r_{ij}$  is the dipole–dipole distance. Assuming the dipoles are aligned with the field of the ion, simple expressions can be obtained for the energies. For model A, taking the same dipole moments and distances yields:  $U_A = -702p/r^2 + 174p^2/r^3$ , where  $p$  is in D,  $r$  in Å, and  $U$  in kT. In model B, again assuming the same dipoles and distances among the neighbors, we get:  $U_B = -318p/r^2 - 194p^2/r^3$ . These

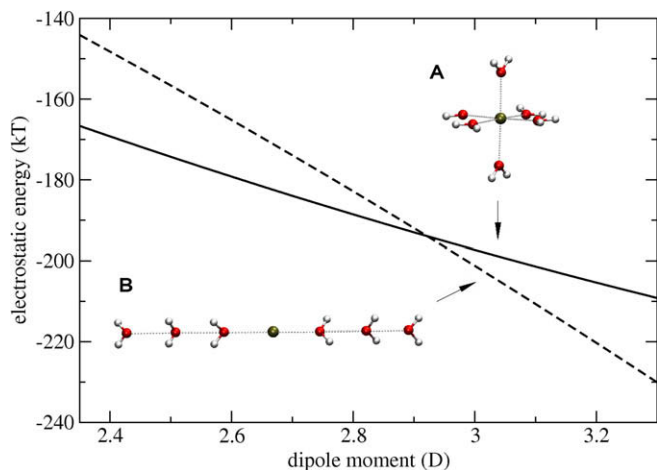


**Fig. 4.** Electrostatic energies of the two model systems representing the  $K^+$  ion-water configurations in bulk (A) and gA (B).

energies are plotted in Fig. 4 against the dipole moment using  $r = 2.8 \text{ \AA}$ .

For a fixed dipole model with  $p = 2.35 \text{ D}$ , the bulk model is seen to be more stable than the chain model by more than 20 kT. With increasing value of  $p$ , however, the energy difference gets smaller and at  $p = 3.0 \text{ D}$ , the chain model becomes more stable. Similar results are obtained using the CHARMM force field and the density functional calculations for the two model systems. Thus use of larger dipole moments for water in polarizable models will help to reduce the energy barrier found in fixed dipole models for translocating an ion from bulk to the channel center. The fact that hydration waters in a pore have larger dipole moments compared to those in bulk should further help in stabilizing a  $K^+$  ion at the center of the gA channel relative to bulk. These results indicate that the large free energy barriers obtained from classical MD simulations are most likely due to using non-polarizable force fields, and use of a properly parametrized polarizable force field should help to resolve this problem.

#### 4. Conclusions

In conclusion, our *ab initio* calculations of water dipole moments indicate a very different behavior for water in narrow pores compared to that in bulk. For pure water, the dipole moments in a pore are suppressed due to loss of hydrogen bonds. In the presence of an ion, however, confinement in a single-file turns into an advantage and leads to an increase in the dipole moment of hydration waters compared to that in bulk. Simple energy estimates obtained from electrostatic calculations indicate that the effect has

the right order of magnitude to resolve the problem of large ionic energy barriers in the gA channel, which arise when non-polarizable force fields are used in the potential of mean force calculations. We believe that narrow pores such as gA and carbon nanotube – and even the simple model systems in Fig. 4 – provide valuable test cases and should be exploited more in the design of new generation of polarizable force fields.

#### Acknowledgements

This work was supported by grants from the Australian Research Council. Calculations were carried out using the SGI Altix clusters at the Supercomputer Facility of the Australian National University (Canberra) and the Australian Center for Advanced Computing and Communications (Sydney).

#### References

- [1] H.M. Jaeger, S.R. Nagel, R.P. Behringer, *Rev. Mod. Phys.* 68 (1996) 1259.
- [2] B. Smit, T.L.M. Maesen, *Chem. Rev.* 108 (2008) 4125.
- [3] H. Rafii-Tabar, *Phys. Repts.* 390 (2004) 235.
- [4] M. Karplus, J. Kuriyan, *Proc. Natl. Acad. Sci. USA* 102 (2005) 6679.
- [5] W.F. van Gunsteren et al., *Angew. Chem. Int. Ed.* 45 (2006) 4064.
- [6] T.W. Allen, T. Bastug, S. Kuyucak, S.H. Chung, *Biophys. J.* 84 (2003) 2159.
- [7] T.W. Allen, O.S. Andersen, B. Roux, *Biophys. Chem.* 124 (2006) 251.
- [8] D. Bucher, S. Rauegi, L. Guidoni, M. Dal Peraro, U. Rothlisberger, P. Carloni, M.L. Klein, *Biophys. Chem.* 124 (2006) 292.
- [9] F.X. Coudert, R. Vuilleumier, A. Boutin, *ChemPhysChem* 7 (2006) 2464.
- [10] Y.Y. Sham, Z.T. Chu, H. Tao, A. Warshel, *Proteins: Struct. Funct. Genet.* 39 (2000) 393.
- [11] H. Guo, N. Gresh, B.P. Roques, D.R. Salahub, *J. Phys. Chem. B* 104 (2000) 9746.
- [12] P. Jungwirth, D.J. Tobias, *Chem. Rev.* 106 (2006) 1259.
- [13] T.M. Chang, X.L. Dang, *Chem. Rev.* 106 (2006) 1305.
- [14] W.L. Jorgensen, *J. Chem. Theor. Comput.* 3 (2007) 1877.
- [15] S.A. Clough, Y. Beers, G.P. Klein, L.S. Rotham, *J. Chem. Phys.* 59 (1973) 2254.
- [16] J.K. Gregory, D.C. Clary, K. Liu, M.G. Brown, R.J. Saykally, *Science* 275 (1997) 814.
- [17] W.L. Jorgensen, J. Chandrasekhar, J.D. Madura, R.W. Impey, M.L. Klein, *J. Chem. Phys.* 79 (1983) 926.
- [18] Y.S. Badyal et al., *J. Chem. Phys.* 112 (2000) 9206.
- [19] R. Car, M. Parrinello, *Phys. Rev. Lett.* 55 (1985) 2471.
- [20] P.L. Silvestrelli, M. Parrinello, *Phys. Rev. Lett.* 82 (1999) 3308.
- [21] T. Todorova, A.P. Seitsonen, J. Hutter, I.F.W. Kuo, C.J. Mundy, *J. Phys. Chem. B* 110 (2006) 3685.
- [22] D. Bucher, S. Kuyucak, *J. Phys. Chem. B* 112 (2008) 10786.
- [23] S. Xantheas, *Chem. Phys.* 258 (2000) 225.
- [24] M. Devereux, P. Popelier, *J. Phys. Chem. A* 111 (2007) 1536.
- [25] D.D. Kemp, M.S. Gordon, *J. Phys. Chem. A* 112 (2008) 4885.
- [26] T. Bastug, A. Gray-Weale, S.M. Patra, S. Kuyucak, *Biophys. J.* 90 (2006) 2285.
- [27] T. Bastug, S. Kuyucak, *Chem. Phys. Lett.* 436 (2007) 383.
- [28] L. Kale et al., *J. Comput. Phys.* 151 (1999) 283.
- [29] A.D. MacKerell Jr. et al., *J. Phys. Chem. B* 102 (1998) 3586.
- [30] A. Laio, J. VandeVondele, U. Rothlisberger, *J. Chem. Phys.* 116 (2002) 6941.
- [31] W. Kohn, L.J. Sham, *Phys. Rev. A* 14 (1965) 1133.
- [32] C.T. Lee, W.T. Yang, R.G. Parr, *Phys. Rev. B* 37 (1988) 785.
- [33] A.D. Becke, *Phys. Rev. A* 38 (1988) 3098.
- [34] N. Trouillier, J.L. Martins, *Phys. Rev. B* 43 (1991) 1993.
- [35] CPMD, MPI für Festkörperforschung, Stuttgart, 1997–2001.
- [36] N. Marzari, D. Vanderbilt, *Phys. Rev. B* 56 (1997) 12847.